Scaling-down lithographic dimensions with block-copolymer materials: 10-nm-sized features with poly(styrene)-block-poly(methylmethacrylate)

Xavier Chevalier, Célia Nicolet, Raluca Tiron, Ahmed Gharbi, Maxime Argoud, Jonathan Pradelles, Michael Delalande, Gilles Cunge, Guillaume Fleury, Georges Hadziioannou, et al.

Scaling-down lithographic dimensions with block-copolymer materials: 10-nm-sized features with poly (styrene)-*block*-poly(methylmethacrylate)

Xavier Chevalier
Arkema France, France and CEA, LETI, Grenoble, France

Célia Nicolet
Arkema France, France and Université Bordeaux I-CNRS LCPO-UMR 5629, Talence, France

Raluca Tiron
Ahmed Gharbi
Maxime Argoud
Jonathan Pradelles
CEA, LETI MINATEC Grenoble, France

Michael Delalande
Gilles Cunge
LTM-CNRS CEA, LETI, Grenoble, France

Guillaume Fleury
Georges Hadziioannou Université Bordeaux I-CNRS LCPO-UMR 5629, Talence, France

Christophe Navarro
Arkema France, France

Abstract. Poly(styrene)-*block*-poly(methylmethacrylate) (PS-*b*-PMMA) block-copolymers (BCP) systems synthesized on an industrial scale and satisfying microelectronic's requirements for metallic contents spec-ifications are studied in terms of integration capabilities for lithographic applications. We demonstrate in particular that this kind of polymer can efficiently achieve periodic features close to 10 nm. These thin films can be transferred in various substrates through dry-etching techniques. The self-assembly optimization for each polymer is first performed on free-surface, leading to interesting properties, and the changes in self-assembly rules for low molecular-weight polymers are investigated and highlighted through different graphoepitaxy approaches. The improve-ments in self-assembly capabilities toward low periodic polymers, as well as the broad range of achievable feature sizes, make the PS-*b*-PMMA system very attractive for lithographic CMOS applications. We con-clude by showing that high-χ polymer materials developed in Arkema's laboratories can be efficiently used to reduce the pattern's size beyond the ones of PS-*b*-PMMA based BCP's capabilities.

Subject terms: lithography; block-copolymer; self-assembly; PS-*b*-PMMA; graphoepitaxy.

1 Introduction

The self-assembly of block-copolymers (BCP) has been identified as an interesting alternative or complementary approach to current advanced lithographic techniques [extreme ultraviolet (EUV), e-beam, optical 193 nm pattern-ing, etc.] in order to decrease further accessible dimensions for microelectronics.[1] Indeed, their abilities to spontaneously form various periodic nanometers-sized structures—such as cylinders or lamellas—render them particularly attractive for dedicated lithographic applications such as line-spaces or contact-holes. Moreover, for several years, researches over BCP's properties highlighted both that the self-assembly may be controlled through guiding prepatterns (the so-called graphoepitaxy[2] or chemi-epitaxy[3] approaches) in order to efficiently increase its long-range order while the ordered

mesostructures inherent to the BCP self-assembly may be formed on a short-time scale compatible with conventional lithographic processes.[4]

However, the self-assembly properties are intimately linked to the chemical nature and architecture of the BCP used. For example, the accessible morphologies of a BCP constituted with three chemically distinct blocks ("ABC" type tri-BCP, "A," "B," and "C" representing each block) are far more numerous when compared to the ones of a simple di-block copolymer.[5] Furthermore, it has been demonstrated that the use of a tri-BCP with an "ABA" architecture (same chemical block at the both extremities of the polymeric chain) may lead to an increase of the time required to reduce defects in the self-assembly when compared to the corresponding simpler di-BCP with the same block-chemistries.[6] A lot of attention has also been paid to the usefulness of BCPs presenting an elevated Flory–Huggins interaction parameter ("χ")—i.e., a strong degree of chains repulsion between each block.[7] The high value of the χ parameter allows the synthesis of BCPs with a lower overall molecular weight, leading directly to smaller BCP features with sharp interfaces between the blocks components. The main drawback of an increased value of the χ parameter is an additional energetic cost for the self-assembly to take place, though the total required energy is lowered through the use of smaller polymeric chains. Therefore, the self-assembly kinetic, depending on the balance of the couple χ value/polymer size, could be reduced for such systems.

Among the various BCP systems reported in the literature, poly(styrene)-*block*-poly(methylmethacrylate) (noted PS-*b*-PMMA) is a well-studied one and presents interesting properties from a technological point of view. First, styrene and methylmethacrylate monomers can be readily copolymerized in the same reactor through nitroxide mediated polymerization—i.e., without metal catalyst—in order to obtain a *random* copolymer (noted PS-*r*-PMMA) with precise composition. This property is extremely valuable since it is limited to only a few monomeric systems, and because *random* copolymers are used as effective "neutral" passivation layer on substrates to properly orient the BCP features.[8] Moreover, the intrinsic chemical nature of both PS and PMMA monomers allows, under appropriate conditions, to synthesize a BCP with well-controlled architecture and composition, and low dispersity of chains distribution. In addition, at elevated temperatures the surface tension of both PS and PMMA are almost equivalent, providing a natural "neutral" interaction between the ambient air and the BCP. Consequently perpendicular BCP features can be obtained without the use of sophisticated systems (solvents atmosphere, vacuum, etc.), which could be potentially prohibitive for lithography. It has also been demonstrated that the self-assembly of a PS-*b*-PMMA system takes place with a simple thermal bake at elevated temperature in a short-time scale, i.e., under similar conditions as classical lithographic processes.[9] Despite those interesting characteristics, a technological debate remains open about the usefulness of this particular system for lithographic applications due to the "small" Flory–Huggins interaction parameter between PS and PMMA, thus limiting the minimum accessible feature's size, though this same "small" χ favors the self-assembly's kinetic of higher molecular-weight polymers.

In this paper, we present our studies on the self-assembly of PS-*b*-PMMA BCP systems exhibiting both lamellar and cylindrical morphologies. Those BCPs are synthesized by Arkema, using anionic polymerization reaction on a semi-industrial scale with a well-controlled reproducibility and low dispersity for various molecular weights and compositions. Self-assembly processes are carefully optimized over a wide range of polymers molecular weights in order to obtain processes largely independent of the thin thickness while satisfying the stringent lithographic requirements (short-time processes, metal-free polymers, etc.). We show in particular that the low molecular weight PS-*b*-PMMA systems can reach perpendicular features with critical dimensions as low as ~10 nm, therefore making such materials very attractive down to the corresponding technological node. Conversely, we show that the high molecular weight BCPs can also be synthesized efficiently to achieve features with natural periods close to ~50 nm, rendering this kind of polymers interesting for an early introduction of BCP technology into current logical-nodes steps. The different morphologies and molecular weights are integrated through various graphoepitaxy approaches to demonstrate the usefulness of those systems for lithography, and the characteristics of each ones are highlighted mainly through the formation of macro-sized polymeric crystals. To further illustrate the usefulness of such polymers for the microelectronic industry, different PS-*b*-PMMA pattern sizes are transferred in the silica, silicon, or lithography-dedicated substrates through dry-etch techniques. Finally, we show that high-χ polymer materials developed in our laboratories can be efficiently used to reduce the pattern's size beyond the ones of PS-*b*-PMMA based BCP's capabilities.

2 Experimental

PS-*b*-PMMA and PS-*r*-PMMA copolymers were synthesized by Arkema, under the tradename Nanostrength EO®. The materials were used as received. Microelectronic grade propylene glycol methyl ether acetate (PGMEA) used in this study was purchased from Rohm&Haas™ and used as received.

Guiding patterns were generated using an e-beam hydrogen silsesquioxane(HSQ) negative tone resist XR-1541 E-Beam Resist, from Dow Corning®. A 40-nm resist thin film was spin-coated on 300 mm silicon wafers on a RF3 Sokudo track. E-beam lithography was performed using a Vistec VSB 3054DW device. The exposure utilizes an accelerating voltage of 50 kV and an exposure dose of 1350 $\mu C/cm^2$. After exposure, samples were developed for 5 min using tetramethylammonium hydroxide (TMAH) at 2.38 wt. %, and then baked at 215°C for 60 s.

PS-*b*-PMMA and PS-*r*-PMMA powders were dissolved in PGMEA to obtain 1 to 2 wt. % solutions. The PS-*r*-PMMA solution was spin-coated on 3×3 cm silicon (100) pieces or prepatterned samples at 700 rpm to obtain thin films of ~90 nm thickness and then annealed at 230°C for 10 min to ensure the chemical grafting. Afterwards, the substrate was thoroughly washed in PGMEA to remove the non-grafted materials. PS-*b*-PMMA solutions were spin-coated on the top of the PS-*r*-PMMA brush layer and annealed on a hotplate at elevated temperature to allow the self-assembly process to take place. Samples with different polymer film thicknesses were generated depending on the processing

parameters such as spin-coating speed or the initial solutions concentration. In a last step, the PMMA domains were selectively removed by acetic acid development and/or O_2 plasma treatment.

The development of the etching processes (random copolymer removal, SiO_2 mask opening, and silicon etching) was performed in an industrial etcher (DPS™ from Applied Materials). The decoupled plasma source (DPS) is an inductively coupled high density plasma source where both the source antennae and the bottom electrode are powered. The source consists of a ceramic dome with an radio frequency three-dimensional coil configuration around it. The bottom electrode is powered through a capacitive coupling at a slightly higher frequency (13.56 MHz) than the source (12.56 MHz). The source power (Ws) controls the ion and reactive neutral species densities, whereas the bottom power (Wb) controls the energy of ions impinging onto the wafer surface. The lower electrode is a monopolar electrostatic chuck (ECS) and the wafer temperature is kept at 50°C by helium backside cooling on the ECS chuck. The Al_2O_3 chamber wall temperature is maintained at 80°C by a heat exchanger while the ceramic dome is air cooled when the plasma is on, and is heated by lamps when the chamber is idle, providing a constant temperature of 60°C.

Top-view SEM pictures were acquired on a CD-SEM H9300 from Hitachi.

3 Results and Discussion

3.1 *Synthesis and Characterizations*

PS-*b*-PMMA with various molecular weights and morphologies (cylindrical or lamellar polymers) used in this study was synthesized in Arkema's facility using sequential anionic polymerization reactions, with a production capacity based on an industrial level. Even with such high-scale type production, the polymer macromolecular characteristics (molecular weight, composition, and dispersity) as shown in Fig. 1 are very well controlled, and their physico-chemical characteristics match well with those of classical laboratory-made BCPs where only few grams of product per batch may be obtained.

The semi-continuous process flow, in combination with the sequential polymerization reaction, used to synthesize the BCP allows for a high-flexibility designed polymeric architecture, in terms of morphologies, composition, and molecular weight. Indeed, this process allows the fine tuning of the final BCP molecular weight and composition during the polymerization reaction to obtain fine different BCPs starting from the same living PS precursor if needed (Fig. 2). This flexibility in the BCP design contributes for the selection of polymeric systems exhibiting improved physico-chemicals characteristics in regards to the self-assembly's properties.

After purification of the raw materials, the level of residual metallic contamination is investigated with inductively coupled plasma-mass spectrometry (ICP-MS) analysis. A typical spectrum representing the content of various metallic cation species in the BCP is shown in Fig. 3. Striking evidence in this spectrum is that the metallic ions content for this kind of BCPs is far below the ones coming from other commercially available polymers. Furthermore, since the content is inferior to 10 ppb for each studied cation for a solution at 2 wt. % of BCP in PGMEA, Arkema's BCPs fully satisfy the current lithographic specifications for CMOS dedicated technologies without any contamination risks for 300 mm tracks. Future improvements in the

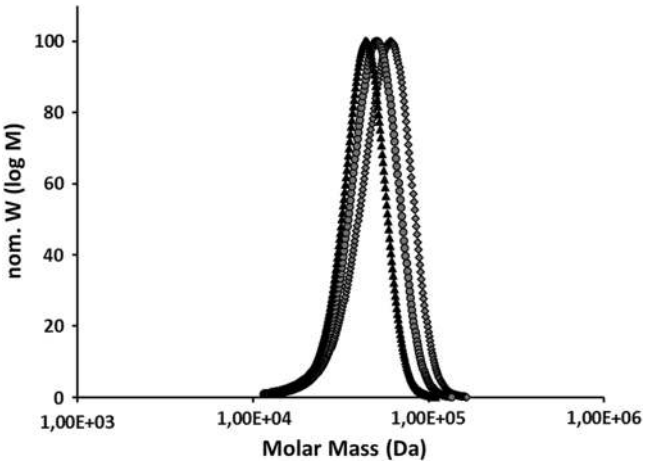

Fig. 2 GPC curves of three BCPs with different molecular weights, synthesized from the same PS-living block.

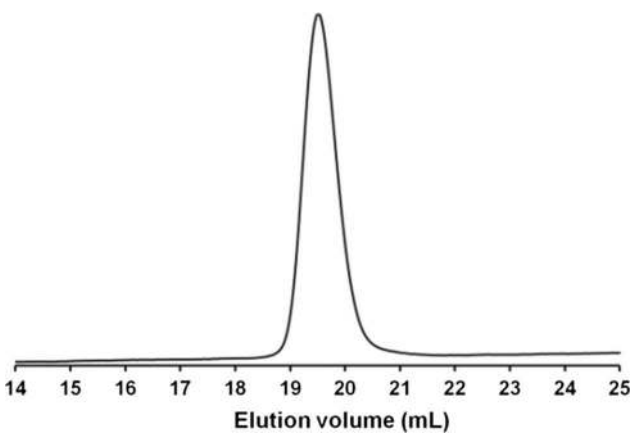

Fig. 1 Typical size exclusion chromatography curve of a PS-*b*-PMMA BCP, synthesized on an industrial scale, exhibiting a molecular chain dispersity of 1.07.

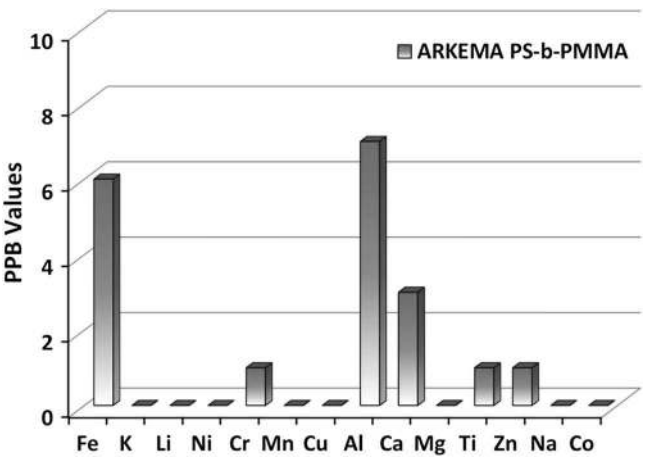

Fig. 3 ICP-MS study showing the low metallic contamination level of a PS-*b*-PMMA BCP after purification.

purification process will lead to lower metallic ions contents, in order to satisfy even harsher specifications.

3.2 *Self-Assembly Optimization*

PS-*b*-PMMA copolymers were designed to target both cylindrical and lamellar morphologies and to obtain a large range of periods. For both morphologies, the self-assembly process (film thickness, surface-energy, temperature, etc.) was tuned to achieve fully perpendicular features without defects. BCP's periods were determined through fast Fourier transform or nearest-neighborsdistance measurements starting from calibrated SEM pictures.

For the cylindrical BCPs used in this study, the smallest period reached at this time was as low as 22 nm, whereas the largest BCP assembly exhibits a period of 51 nm with a progressive increment for the BCP period over the range of molecular weight (Fig. 4). In the case of lamellar BCPs, the smallest period obtained was 19 nm [leading to critical dimension (CD) inferior to 10 nm], and the largest one reached 37 nm (Fig. 5). For both morphologies, the periods shown here are surely not the ultimate ones that PS-*b*-PMMA-based polymers may achieve, and current works are in progress in order to further lower and enlarge the accessible periods with these polymers. Anyway, both lamellar and cylindrical periods reported here demonstrate that this kind of polymers may be efficiently used as thin films to create nanolithographic masks with CDs close to 10 nm, rendering such systems attractive candidates down to this corresponding technological node. It is interesting to note also that fully perpendicular cylindrical features can be obtained for periods close to 51 nm. Such high polymeric periods are potentially interesting for an early introduction of BCP self-assembly in lithographic applications (for contact shrink ones as example) in the current nodes.

The self-assembly process parameters of all polymers were optimized in order to fit with current lithographic process constraints (short PS-*r*-PMMA grafting time, short bake-time, temperatures, and solvent compatible with 300 mm tracks, etc.). The fine tuning in BCP's composition during the synthesis allowed us to select PS-*b*-PMMA systems with very interesting properties. Indeed, some of them exhibit e.g., very weak dependence toward the BCP filmthickness: the BCP self-assembly was performed with a 5 nm increment in film thickness as shown in Fig. 6 (all the pictures are not reported here), starting from 20 up to 270 nm, and the polymer exhibits a fully perpendicular cylindrical structure without any defects (in-plane cylinders, etc.) over the whole range of thicknesses. The tomography of these thick films was performed by successive gentle etching of the films with O_2-based plasmas (Fig. 7). The SEM pictures obtained after each etching step prove clearly that the perpendicular order of the cylinders propagates through the whole film thickness without apparent defects.

In the same way, another interesting characteristic for lithographic applications may be the low sensibility of the perpendicular self-assembly toward the surface energy (PS-*r*-PMMA composition used for substrate modification).

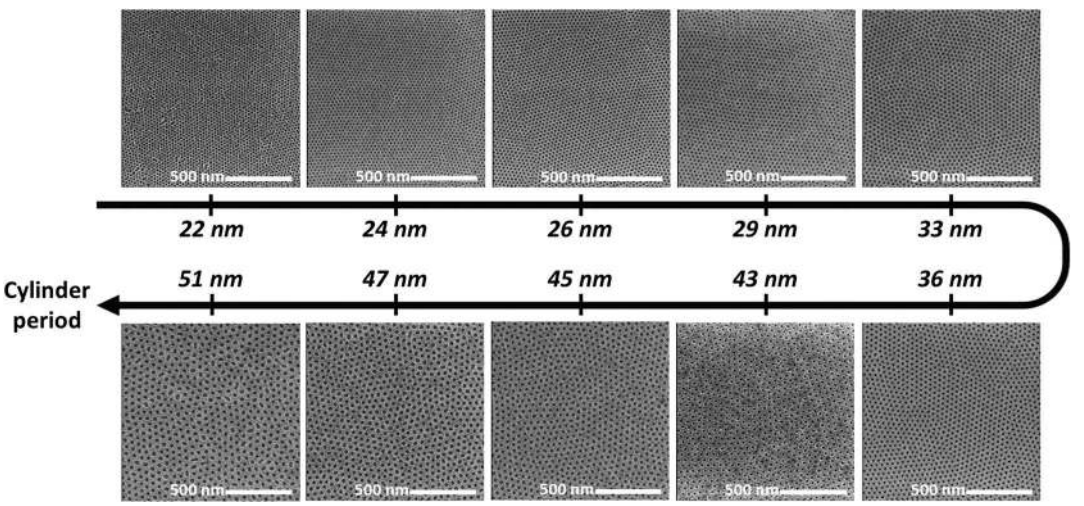

Fig. 4 SEM top-view pictures illustrating the perpendicular self-assembly of various PS-*b*-PMMA cylindrical BCPs (PMMA cylinders in a PS matrix) with periods ranging from 22 up to 51 nm.

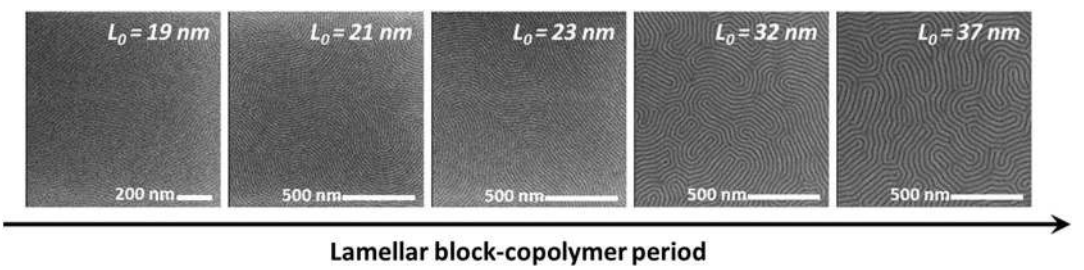

Fig. 5 SEM pictures showing the perpendicular self-assembly of lamellar BCPs with periods ranging from 19 up to 37 nm.

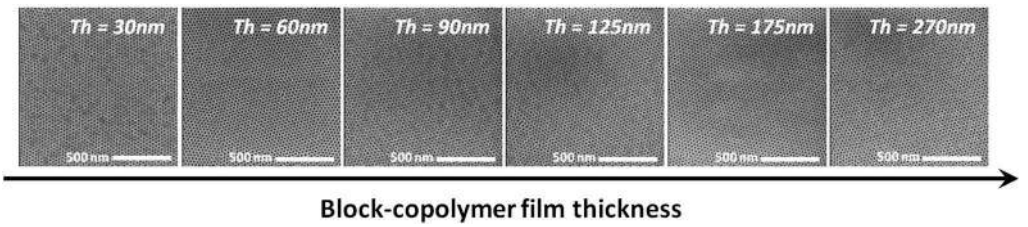

Fig. 6 Scheme of SEM pictures illustrating the weak dependence between a BCP and its film thickness.

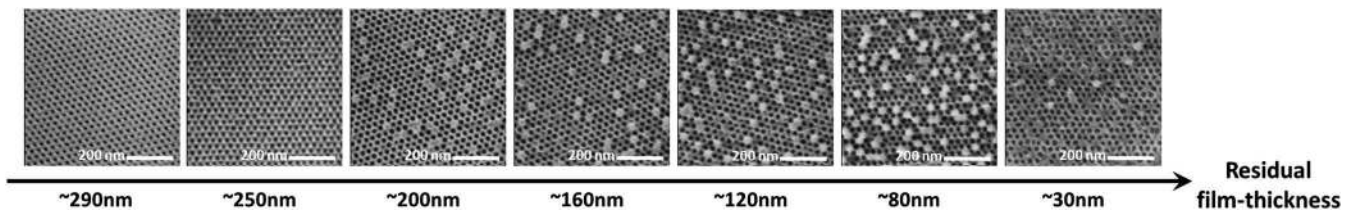

Fig. 7 Stepwise O_2 plasma etching of a BCP film having an initial thickness of ~290 nm demonstrating that the perpendicular cylindrical morphology propagates throughout the whole film thickness.

To illustrate this property, the SEM pictures displayed in Fig. 8 show a polymer with perpendicular cylindrical structure for very different PS contents in PS-*r*-PMMA (the variation in PS content between "%PS1" and "%PS3" is close to 25%), although few defects appear for specific BCP film thickness. This can be used to alleviate the use of *random* copolymers with a specific composition to obtain perpendicular self-assembled structure, enlarging therefore the BCP's process-window available for lithography.

The BCP's self-assembly process optimization becomes extremely important for low molecular-weight polymers. Indeed, the order–disorder transition temperatures (T_{ODT}) for these particular systems are quite low and the high-temperature bake inherent to the self-assembly process cannot be maintained for small PS-*b*-PMMA without presenting the risk to exceed the T_{ODT} of the system, leading to featureless structures. It is rather an advantage for PS-*b*-PMMA polymers self-assembly for small lithographic dimensions since the decrease in bake temperatures will contribute to a reduction in process costs. This is not the sole advantage in the use of small PS-*b*-PMMA polymers for lithography. Some other ones, linked to graphoepitaxy approach, will be described in Sec. 3.3. The dependence of the self-assembly process as regards to the temperature is illustrated in Fig. 9, where the classical 240 to 250°C (or more) process temperature has to be modified for this 19-nm period lamellar polymer: at constant process time, both 160 and 200°C bakes lead to poorly ordered partially perpendicular structures, while well-ordered lamellas appear for a temperature close to 180°C. The fact that the lamellas are not well featured at 160°C

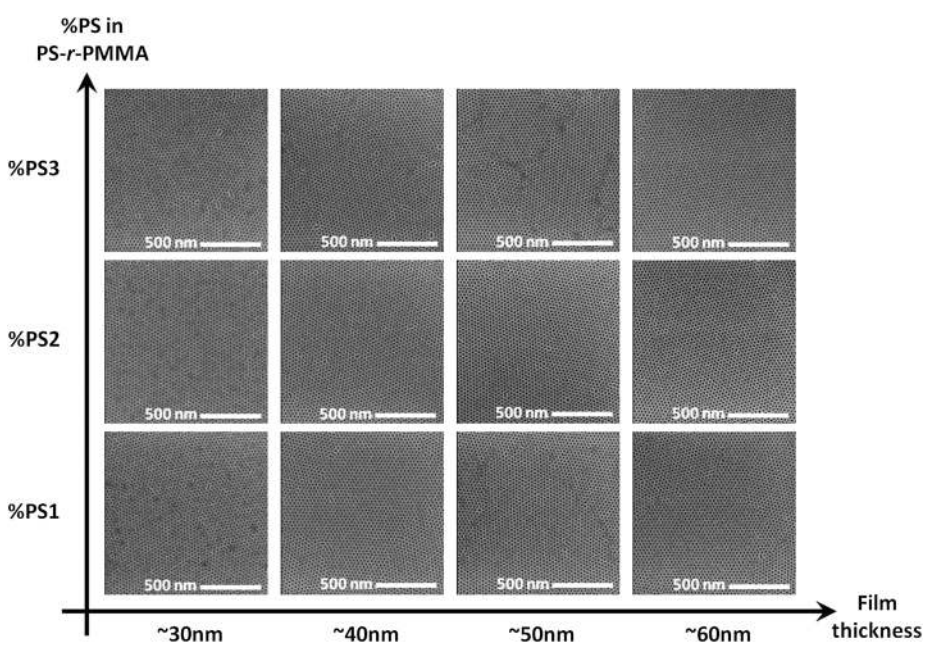

Fig. 8 Self-assembly of a BCP with different film-thickness on various PS-*r*-PMMA with different PS contents showing that weak surface-energy dependence may be achieved.

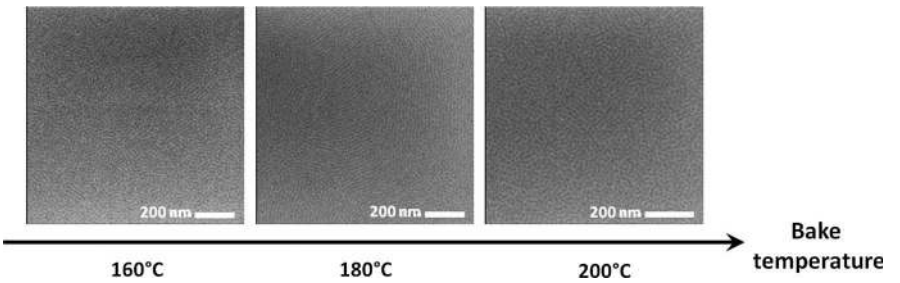

Fig. 9 Self-assembly of a low molecular weight lamellar PS-*b*-PMMA BCP presenting a T_{ODT} close to 190°C illustrating the fact that the process parameters must be carefully tuned to reach an optimal order.

is due to a slowed self-assembly's kinetic (due to the high T_g of PMMA and PS), while at 200°C (and 190°C) the PS and PMMA chain segments become miscible leading to the loss of the order parameter. We therefore located the T_{ODT} of this polymer between 180 and 190°C and recently demonstrated this value by DMA measurements at low shearing rate.

It is interesting to note also that T_{ODT} of PS-*b*-PMMA BCPs are now accessible with these small polymers, whereas it is usually located above the degradation point for more classical BCPs. The location of the T_{ODT} for well-calibrated molecular weights and morphologies will lead to interesting information sets for self-assembly of PS-*b*-PMMA-based polymers, but this is beyond the scope of this study and these results will be reported elsewhere.

A dry-etching procedure was already reported in previous publications in order to transfer the BCP mask in the bulk silicon or substrates of interest for lithography such spin-on-carbon (SOC), through a sacrificial silica hard-mask methodology leading to nice aspect-ratio features.[10,11] This procedure contains three main steps: a first step consists of the PS-*r*-PMMA layer removal with a short Ar/O_2 plasma, followed by the transfer of the BCP features in the silica hard-mask layer with a fluorocarbon-based plasma, and these silica structures are finally transferred in the bulk silicon with an $HBr/Cl_2/O_2$ plasma. The same approach is kept for the SOC substrate: after the step of brushes opening with an Ar/O_2 plasma, the features are transferred in the SiARC hard-mask with fluorocarbon chemistry, and then in the SOC with an O_2 plasma. Figure 10(a) and 10(b) show that a 36-nm period BCP can be efficiently transferred in bulk silicon as well as in SOC substrate, respectively, with high aspect ratio features. Figure 10(c) shows that the 28-nm period BCP mask may be successfully transferred in the 10-nm thick silica hard-mask, leading to features with a mean CD close to 11 nm. Although the dry transfer process is still under improvement, one has to mention that the PS-*r*-PMMA opening step is critical to avoid an exceeding enlargement of the final CD.[12] Anyway, as the BCP's period used here is not the smallest one available, final CD (after etch-transfer) could efficiently reach dimensions close to or below 10 nm with PS-*b*-PMMA BCPs.

3.3 *Graphoepitaxy Approaches*

Various approaches have been studied over several years in order to improve the correlation length of the BCP self-assembly. Among them, the so-called chemi-epitaxy, using patterns based on chemical contrasts[3] and the graphoepitaxy[2] which uses physical templates (e.g., lithographic resists hard-walls), are both well-known methods to efficiently guide the BCP self-assembly. The improvement of these two techniques leads to their recent introduction in 300-mm tracks as BCP tests structures, chemi-epitaxy for line-space applications,[13] and graphoepitaxy for contact-hole shrink applications in lithography.[14] Both of these methods may present some issues: chemi-epitaxy offers, e.g., some ease of processing, but suffers somewhat of a low capacity in density multiplication of prepatterns since there is no lateral constrain to guide the BCP, while graphoepitaxy presents this efficient lateral strain, but the prepatterns have to resist to solvents or high-temperature bake used for the BCP process.

Our previous studies focused on the graphoepitaxy approach since it starts from an already existent prepattern generated with well-established conventional lithographic techniques (optical or mask-less), and that the BCP self-assembly process is compatible with many substrates/materials.[15] We also demonstrated that this method can be used efficiently to create real two-dimensional (2-D) macroscopic BCP crystals with long-range order (like those obtained viachemi-epitaxy) if the commensurability conditions between the BCP-lattice and the prepattern are well respected.[16]

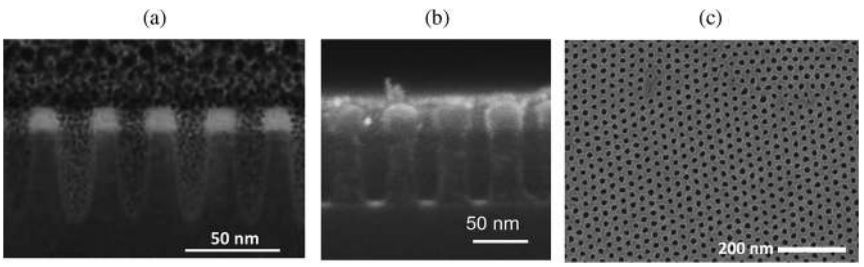

Fig. 10 (a and b) A 36-nmperiod BCP transferred in bulk silicon and SOC substrate, respectively (the upper white areas are the remaining SiO_2 and SiARC hard-masks, respectively). (c) A 10-nm thick silica hard-mask after dry etch-transfer of a PS-*b*-PMMA BCP leading to features with CD close to 11 nm.

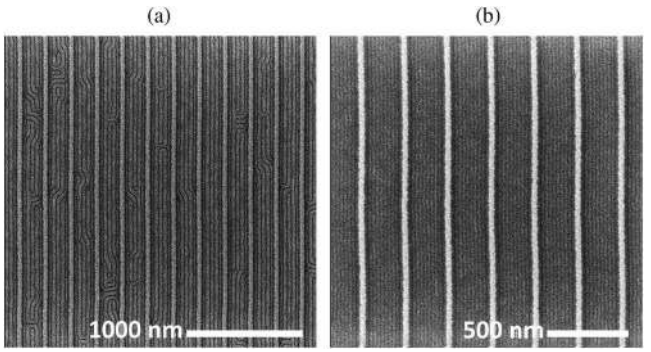

Fig. 11 Graphoepitaxy of two lamellar BCPs having different molecular weights illustrating the increase in ordering for a low molecular weight BCP (b) when the same self-assembly process with a higher molecular weight (a) one is done (white lines: HSQ template).

For practical reasons, the prepatterns used in this study were made with e-beam lithography with a HSQ-based resist, though self-assembly rules depicted here would work for others patterning methods and materials. The SEM pictures in the Fig. 11 show "classical" (i.e., BCP's film thickness below the height of the HSQ lines) graphoepitaxy samples obtained with two lamellar BCPs having different intrinsic periods. An important point to notice is that the self-assembly processes used for these two samples are entirely equivalent; the bake time used was deliberately short (a few minutes) in order to fit those of usual lithographic materials. A striking difference between these two samples is the quality of the BCP's self-assembly. Indeed, Fig. 11(a) shows the assembly of the high molecular weight BCP where many defects are visualized (jogs, broken BCP lines, etc.) although the commensurability conditions were respected in order to obtain three standing-up lamellas. Conversely, the picture resulting from the self-assembly of the small period BCP [Fig. 11(b)] shows eight perfectly aligned standing-up lamellas without defects. Such contrast between the assemblies obtained with these two polymers is solely due to the difference in polymer molecular weight: the smaller the polymer is, the faster the self-assembly's kinetic is (the faster it reaches its equilibrium state). Although not reported here, the same effect has been observed in the case of standing-up cylindrical BCP features. Therefore, the use of small molecular weight PS-*b*-PMMA polymers could be extremely valuable and interesting for lithography since it allows for faster self-assembly processes (phase separation, kinetic of defects reduction, etc.) leading to an increased density multiplication potential.

The "classical" graphoepitaxy approach leads to a one–dimensional (1-D) long-range order, each template being independent from the others, and each resist line being separated from the next one by a few hundred nanometers. The 1-D order may be transformed into a 2-D order by overlayering the polymer's film thickness above the pattern height and controlling carefully the commensurability conditions between the pattern's size and the BCP. This method has been demonstrated with perpendicular cylindrical BCP features leading to perfectly ordered macroscopic polymer crystals.[16]

We show here that this particular method can also be used efficiently with small molecular weights cylindrical BCPs having CD close to 10 nm. The benefit in the use of small molecular weight BCP is an increase in the degree of freedom concerning the prepattern design. Indeed, as in the case of "classical" graphoepitaxy, BCPs having a small period tolerate wider patterns and wider grooves without losing a perfect order. Since here the defect level occurs primarily on the top of the patterns (no lateral strain for the BCP: the order is imposed by the pattern width and the polymer in the grooves), the assembly of a low molecular weight BCP allows for a wider pattern to be used without loss of ordering. This property is illustrated in Fig. 12(b), where six rows of cylinders are present on the top of the HSQ-lines with a high degree of order for the macro-crystal obtained.

Another interesting case is the combination of this method with lamellar BCPs. Indeed, the SEM pictures displayed in Fig. 12(c) and 12(d) show that an increase in the film thickness of the lamellar BCP above the prepattern height leads to a 2-D long-range order: both lamellas in the grooves and the resistlines guide the lamellas located above the HSQ lines providing in this way a macroscopic-sized BCP crystal over the whole prepatterned area. As seen for cylindrical BCPs, the use of a low molecular weight lamellar BCP leads to more freedom in the prepattern design due to the enhancement in their self-assembly kinetic.

One promising application for BCPs to find a place in lithographic industrial processes is the contact-shrink approach:[17] starting from a large round prepattern, the BCP fills this hole with one or several perpendicular cylinders in the middle. Given that current advanced lithographic tools enable the generation of prepattern CD around 60 nm, and that the CD of a BCP cylinder fitting this pattern is around 20 nm, it would allow in fine to divide the initial pattern's size at least by three, leading therefore to an efficient decrease in the initial hole-size for vias application. We show here that PS-*b*-PMMA polymers properties are well adequate for this kind of application, since the prepattern's size may range from ∼70 down to 45 nm with different polymers, without pushing the BCP system toward its lowest limits (Fig. 13). One should refer the reader to another of these

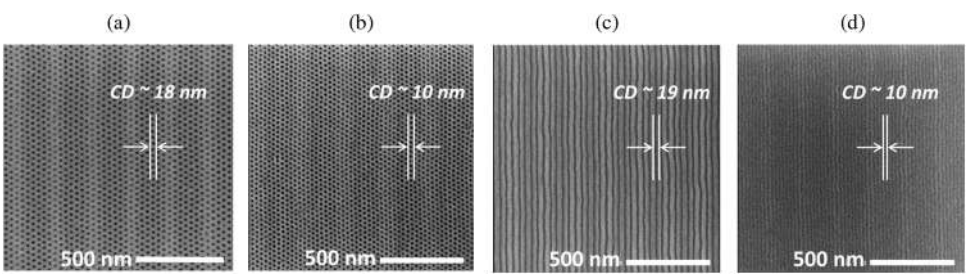

Fig. 12 Macroscopic-sized BCPs crystals obtained from a high molecular weight cylindrical BCP (a) and a low molecular weight cylindrical BCP (b), a high molecular weight lamellar BCP (c) and a low molecular weight lamellar BCP (d) (lighter gray areas: BCPs above the HSQ-resist lines).

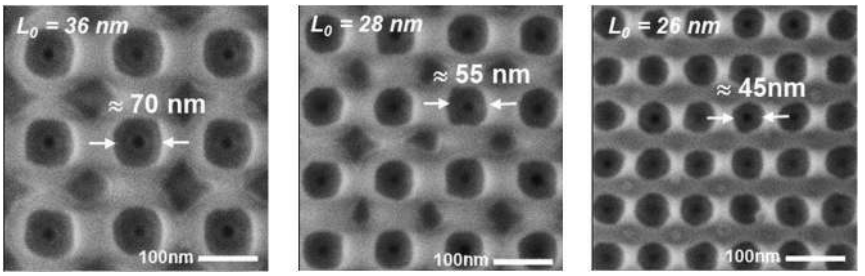

Fig. 13 Various prepatterned contact-hole sizes shrunk with different PS-*b*-PMMA BCPs having periods of 36, 28, and 26 nm, respectively.

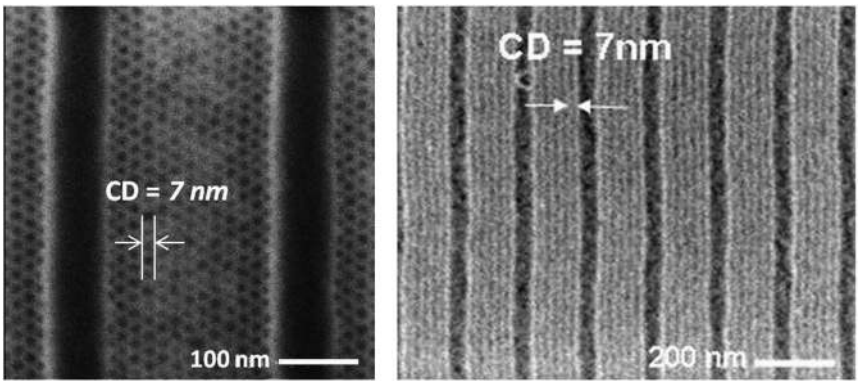

Fig. 14 SEM pictures of high-χ BCPs self-assembled within graphoepitaxy approach (HSQ templates) leading to features down to 7 nm.

proceeding for further details about the potential of such BCPs for this particular application.[13]

3.4 *High-χ Materials*

Despite that PS-*b*-PMMA polymers present interesting properties, achievable CDs with this system will not decrease far below 10 nm due to its relatively low value of Flory–Huggins parameter. To address this specific problem, BCP chemical systems with higher χ values have to be developed, along with their self-assembly processes. The SEM pictures displayed in Fig. 14 demonstrate that BCP features close to 7 nm may be reached with such new polymer systems, and that they can be efficiently guided with traditional graphoepitaxy approach. These results illustrate well the usefulness and capabilities of BCP materials to scale down dimensions of future interest for lithographic applications.

4 Conclusions

We have shown in this paper that PS-*b*-PMMA copolymers systems can be produced efficiently at the industrial scale in a controlled manner with well-defined architectures and without metallic contaminant to fulfill the future needs of microelectronics. The interest of such BCP system relies on the broad range of achievable periodic features exhibiting increased self-assembly capabilities when moving toward low molecular-weight polymers. Despite its "small" χ value, this system is able to produce CDs close to 10 nm and the transfer in the substrate of these features can be done with conventional dry-etching techniques, although the process has still to be improved. Further, CDs scaling down below 10 nm can be achieved efficiently with high-χ BCP materials from Arkema.

Acknowledgments

The authors thank J. Bustos and J. Belledent for the design of HSQ-based templates. This work has been performed under the framework of the IDEAL program involving the different partners.

References

1. The International Technology Roadmap for Semiconductors, http://www.itrs.net/Links/2011ITRS/2011Chapters/2011ERM.pdf (2011).
2. R. A. Segalman et al., "Graphoepitaxy of spherical domain block copolymer films," *Adv. Mater.* **13**(15), 1152–1155 (2001).
3. S. O. Kim et al., "Epitaxial self-assembly of block copolymers on lithographically defined nanopatterned substra," *Nature* **424**(6947), 411–414 (2003).
4. H.-C. Kim et al., "Block copolymer based nanostructures: materials, processes, and applications to electronics," *Chem. Rev.* **110**(1), 146–177 (2010).
5. W. Zheng et al., "Morphology of ABC triblock copolymers," *Macromolecules* **28**(21), 7215–7223 (1995).
6. S. Ji et al., "Directed assembly of non-equilibrium ABA triblock copolymer morphologies on nanopatterned substrates," *ACS Nano* **6**(6), 5440–5448 (2012).
7. Y. S. Jung et al., "Orientation-controlled self-assembled nanolithography using a polystyrene-polydimethylsiloxane block copolymer, *Nano Lett.* **7**(7), 2046–2050 (2007).
8. P. Mansky et al., "Controlling polymer-surface interactions with random copolymer brushes," *Science* **275**(5305), 1458–1460 (1997).
9. A. M. Welander et al., "Rapid directed assembly of block copolymer films at elevated temperatures," *Macromolecules* **41**(8), 2759–2761 (2008).
10. X. Chevalier et al., "Study and optimization of the parameters governing the block copolymer self-assembly: toward a future integration in lithographic process," *Proc. SPIE* **7970**, 79700Q (2011).
11. T. Chevolleau et al., "Self-assembly patterning using block copolymer for advanced CMOS technology: optimisation of plasma etching process," *Proc. SPIE* **8328**, 83280M (2012).

12. X. Gu et al., "High density and large area arrays of silicon oxide pillars with tunable domain size for mask etch applications," *Adv. Mater.* **24**(40), 5505–5511 (2012).
13. C. Bencher et al., "Self-assembly patterning for sub-15nm half-pitch: a transition from lab to fab," *Proc. SPIE* **7970**, 79700F (2011).
14. R. Tiron et al., "The potential of block copolymer's directed self-assembly for contact hole shrink and contact multiplication," *Proc. SPIE* **8680**, 868012 (2013).
15. R. Tiron et al., "Pattern density multiplication by direct self assembly of block copolymers: toward 300mm CMOS requirements," *Proc. SPIE* **8323**, 83230O (2012).
16. R. Tiron et al., "Optimization of block copolymer self-assembly through graphoepitaxy: a defectivity study," *J. Vac. Sci. Technol. B* **29**, 06F206 (2011).
17. J. Y. Cheng et al., "Simple and versatile methods to integrate directed self-assembly with optical lithography using a polarity-switched photoresist," *ACS Nano* **4**(8), 4815–4823 (2010).